



A Combined Crystal-Structural, IR, Raman and ³¹P NMR Spectroscopy of a new iron phosphate FePb₂(P₂O₇)(PO₄)

I. Maarouf^{1*}, A. Oulmekki¹, J. Toyir², F. Lefebvre³, A. Harrach¹, M. Ijjaali¹

¹Laboratoire de Chimie de la matière condensée, Faculté des Sciences et Techniques Fès, Université Sidi Mohammed Ben Abdellah, BP. 2202 Maroc

²Equipe de recherche en procédés pour l'énergie et l'environnement, Laboratoire de Chimie de la matière condensée, Faculté polydisciplinaire Taza, Université Sidi Mohammed Ben Abdellah, B.P. 1223 Taza Maroc.

³Université Lyon1, CPE Lyon, CNRS, UMR C2P2, LCOMS, 43 Bd du 11 Nov. 1918 Villeurbanne, France

Received 8 Jan 2017
Revised 16 Apr 2017
Accepted 18 Apr 2017

Keywords

- ✓ M-P-O,
- ✓ Iron,
- ✓ IR,
- ✓ Raman,
- ✓ Crystal-Structural,
- ✓ ³¹P NMR,
- ✓ Mössbauer.

*maaroufismail@gmail.com
Phone: +212 6 74 78 71 91

Abstract

FePb₂(P₂O₇)(PO₄) has been synthesized using Fe(NO₃)₃·9H₂O, Pb(NO₃)₂ and NH₄H₂PO₄ as starting materials. Single crystals were grown by a long annealing (4 days) at 900°C in open air. FePb₂(P₂O₇)(PO₄) crystallizes in the monoclinic space group P2₁/c, with a=6.484(1) Å, b=7.116(1) Å, c=19.531(1) Å, β=99.31(1)°, and Z=2. The FePb₂(P₂O₇)(PO₄) structure can be described as a three-dimensional array containing isolated [Fe³⁺O₆] octahedra connected through PO₄ tetrahedra and P₂O₇ groups, enclosing a network of cavities where the lead cations reside. IR and Raman characterization of new phosphate FePb₂(P₂O₇)(PO₄) revealed the existence of isolated PO₄³⁻ and P₂O₇⁴⁻ groups from each others, and FeO₆ and PbO_n groups in which the Fe-O and Pb-O bonds are of lower intensity than that of P-O. By comparing the frequencies values between IR and Raman spectrums of FePb₂(P₂O₇)(PO₄), we can conclude that the correlation effect is more important than the site effect. The analysis of the ³¹P NMR spectrum in the solid state of phosphate FePb₂(P₂O₇)(PO₄) confirms the presence of PO₄³⁻ and P₂O₇⁴⁻ groups in agreement with the results determined by crystallography, IR and Raman. The study by Mössbauer spectroscopy allowed us to characterize the degree of oxidation of the iron, its environment in the structure and in particular the covalent Fe-O bonds.

1. Introduction

Phosphates of transition metals have attracted considerable attention and continue to be a subject of many investigations, both in practical and fundamentals aspects [1]. Due to their chemical and physical properties, many phosphates exhibit interesting properties such as heterogeneous catalysis [2], ionic exchange [3], optical applications [4] and so on.

The solid-state chemistry of polyphosphates in which the transition metals exhibits a trivalent oxidation state is traditionally considered unusual [5]. The great ability of the phosphate frameworks to stabilize these oxidation states is produced for the relatively high charge in (PO₄)³⁻ tetrahedra that favors the formation of anionic frameworks with a high degree of mechanical, and thermal stability [6,7]. According to Gleitzer [1] the interest in the diphosphates is also related to the geometry of the P-O-P bridge which is related to the bond order and hence to the overlap of the available oxygen and phosphorus orbitals [1].

Due to these reasons, a great effort, during the past years, has been devoted to the study of mixed valent transition metals phosphates. The Fe-P-O system has been widely studied, and the phase relationships established, at 900°C, by Malaman et al [8]. In the present paper related with investigations of the Fe-Pb-P-O system, we have discovered the first example of iron III lead phosphate: FePb₂(P₂O₇)(PO₄). To our knowledge, only a limited number of phosphates of iron and lead have been reported so far [9,10].

FePb₂(P₂O₇)(PO₄) material was characterized by various spectroscopic techniques: IR, Raman and NMR ³¹P leading to concordant properties of the mixed phosphate material as discussed below.

Numerous researchers have applied the ^{57}Fe Mössbauer spectroscopy, which is known as a structural sensitive technique, on a great number of Fe-based crystals and amorphous materials. The spectroscopy Mössbauer ^{57}Fe was used in order to clarify the valence and local coordination state of iron ions in a new iron phosphate $\text{FePb}_2(\text{P}_2\text{O}_7)(\text{PO}_4)$ crystals.

2. Experimental

$\text{FePb}_2(\text{P}_2\text{O}_7)(\text{PO}_4)$ has been obtained by mixing aqueous solutions of $\text{Fe}(\text{NO}_3)_3 \cdot 9\text{H}_2\text{O} + 2\text{Pb}(\text{NO}_3)_2 + 3\text{NH}_4\text{H}_2\text{PO}_4$. The solution has been evaporated to dryness and the residue has been slowly annealed in air to 400°C and kept at this temperature for 24h, in order to eliminate NH_3 and H_2O . In a second step, the finely ground product has been heated at 700°C for 24h and finally sintered at 800°C for 48h in the open air and quenched to room temperature. From the obtained powders, crystals have been grown by a long annealing (4 days), in gold crucibles, at 850°C in the open air. A single crystal ($100\mu\text{m}$) was selected for the structure determination. The data were collected on CAD4 diffractometer. The Fourier Transform Infra-Red FTIR spectra were recorded using FTIR spectrophotometer (Bruker, Vertex 70), in the range of $4000 - 400\text{ cm}^{-1}$. 16 scans were accumulated at a resolution of 4 cm^{-1} . The Raman spectroscopy analysis was carried out using a Raman SENTERRA system (Bruker) equipped with a laser at 785 nm, an integration time of 20 s and a laser power of 10 mW at the source for a range from 200 to 1200 cm^{-1} . The Mössbauer data have been collected with a constant acceleration spectrometer with 1024 channels. Isomer shifts are reported with respect to α -iron at room temperature. The Mössbauer effect data were analyzed by using least-square minimization techniques [11] to evaluate the hyperfine spectral parameters. The ^{31}P NMR spectra were recorded on a Bruker MSL-300 spectrometer operating at 121.4 MHz. The pulse length was $2\mu\text{s}$. The delay between scans was 100s. The number of scans is 100.

3. Results and discussion

3.1. Crystallographic data

$\text{FePb}_2(\text{P}_2\text{O}_7)(\text{PO}_4)$ crystallizes in the monoclinic system, space group $\text{P}2_1/\text{c}$, with $a=6.484(1)\text{ \AA}$, $b=7.116(1)\text{ \AA}$, $c=19.531(1)\text{ \AA}$, $\beta=99.31(1)^\circ$, and $Z=2$. The crystal structure of $\text{FePb}_2(\text{P}_2\text{O}_7)(\text{PO}_4)$ is built up from corner-sharing between isolated FeO_6 octahedra and PO_4 and P_2O_7 groups, enclosing a network of cavities where the lead cations (Pb^{2+}) reside (Figure 1). The Fe^{3+} octahedra is almost regular with average distance of $2.034(2)\text{ \AA}$. This distance is comparable with those reported for other phosphates (e.g., II- NaFeP_2O_7 , $\text{Fe-O}=1.99\text{ \AA}$ [12] ; $\text{KbaFe}_2(\text{PO}_4)_3$, $\text{Fe}_1\text{-O}=1.99\text{ \AA}$ and $\text{Fe}_2\text{-O}=2.01\text{ \AA}$ [13]) ; $\text{Na}_7\text{Fe}_4(\text{PO}_4)_6$ [14], $\text{Fe}_1\text{-O}=2.06\text{ \AA}$ and $\text{Fe}_2\text{-O}=2.08\text{ \AA}$; $\text{PbFe}_2(\text{P}_2\text{O}_7)_2$, $\text{Fe-O}=1.99\text{ \AA}$ [10]; $\text{SrFe}_2(\text{P}_2\text{O}_7)_2$, $\text{Fe-O}=1.99\text{ \AA}$ [10])

The iron atoms are gathered in FeO_6 octahedra connected to each other by pyrophosphate groups (Fe-O-P-O-Fe bonds). The Fe-Fe distances varying from 5.4 to 5.8 \AA .

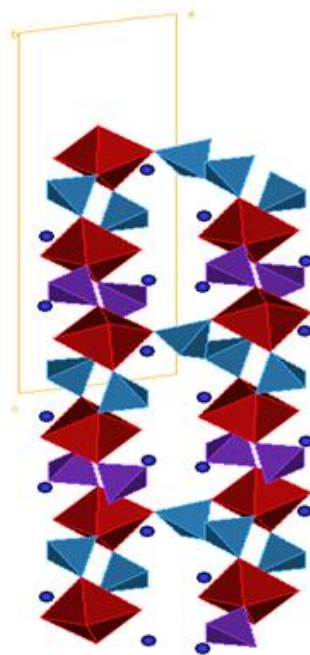


Figure 1: The projection of $\text{FePb}_2(\text{P}_2\text{O}_7)(\text{PO}_4)$ structure on the plane (010).

3.2. Vibration analysis of $\text{FePb}_2(\text{P}_2\text{O}_7)(\text{PO}_4)$ using IR and Raman.

3.2.1. Vibration analysis using site method

Basically, the so-called site method [15-17] is consisting in three key steps: (i) determination of the irreducible representations of the molecular group, (ii) association of the molecular group to the site group and (iii) ascribing of the site group to the point group. The site group (Gs) is defined by the set of operations that can achieve the crystal symmetry elements intersecting at the center of molecule.

Following this method, it is found that the structure of $\text{FePb}_2(\text{P}_2\text{O}_7)(\text{PO}_4)$ is characterized by the existence of PO_4^{3-} and $\text{P}_2\text{O}_7^{4-}$ groups isolated from each others, and the presence of FeO_6 and PbO_n groups. Application of the site method tools for predicting the potential vibration modes leads to two types of vibrations:

- Internal for PO_4^{3-} and $\text{P}_2\text{O}_7^{4-}$ groups
- External for PO_4^{3-} and $\text{P}_2\text{O}_7^{4-}$ groups and Fe^{2+} and Pb^{2+} cations.

Resulting correlations of PO_4^{3-} and $\text{P}_2\text{O}_7^{4-}$ ions in $\text{FePb}_2(\text{P}_2\text{O}_7)(\text{PO}_4)$ crystals are shown in Tables 1 and 2.

Table 1: Correlation diagram of PO_4^{3-} ions in $\text{FePb}_2(\text{P}_2\text{O}_7)(\text{PO}_4)$ crystals.

Normal vibration modes of isolated PO_4^{3-} (Td)	Td Molecular Group	C_1 site group	C_{2h} factor group
1 v 1	$\text{A}_1(\text{Ra})$	$9 \text{ A} (\text{Ra}, \text{IR})$	9 Ag (Ra)
1 v 2	$\text{E}(\text{Ra})$		9 Bg (Ra)
2 (v3, v4)	$2\text{T}_2(\text{IR}, \text{Ra})$		9 Au (IR)
			9Bu (IR)

v 1, v 2, v 3, v 4 are the normal modes of the fundamental vibration of ion PO_4^{3-} according to Hezberg notation [18].

Examination of Table 2 shows the presence of 36 internal vibrations of the ion PO_4^{3-} in C_{2h} factor group, the representation of these vibrations is given by:

$$\Gamma_{\text{PO}_4}^{\text{PO}_4}(\text{internal}) = 9 \text{ Ag} (\text{Ra}) + 9 \text{ Bg} (\text{Ra}) + 9 \text{ Au} (\text{IR}) + 9\text{Bu} (\text{IR})$$

Table 2: Correlation diagram of $\text{P}_2\text{O}_7^{4-}$ ions in $\text{FePb}_2(\text{P}_2\text{O}_7)(\text{PO}_4)$ crystals.

Molecular Group C_{2v}	C_1 site group	C_{2h} factor group
7 $\text{A}_1(\text{Ra}, \text{IR})$	$21 \text{ A}(\text{Ra}, \text{IR})$	21 Ag (Ra)
4 $\text{A}_2(\text{Ra})$		21 Bg (Ra)
6 $\text{B}_1(\text{Ra}, \text{IR})$		21 Au (IR)
4 $\text{B}_2(\text{Ra}, \text{IR})$		21 Bg (IR)

Examination of Table 3 shows the presence of 84 internal vibrations of the ion $\text{P}_2\text{O}_7^{4-}$ in C_{2h} factor group, the representation of these vibrations is given by:

$$\Gamma_{\text{P}_2\text{O}_7}^{\text{P}_2\text{O}_7}(\text{internal}) = 21 \text{ Ag} (\text{Ra}) + 21 \text{ Bg} (\text{Ra}) + 21 \text{ Au} (\text{IR}) + 21 \text{ Bg} (\text{IR})$$

In the following section, we carried out the IR and Raman spectroscopy experimental analysis of $\text{FePb}_2(\text{P}_2\text{O}_7)(\text{PO}_4)$.

3.2.2. Experimental vibration spectrums of $\text{FePb}_2(\text{P}_2\text{O}_7)(\text{PO}_4)$

a-Infrared absorption spectrum of $\text{FePb}_2(\text{P}_2\text{O}_7)(\text{PO}_4)$

The infrared (IR) absorption spectrum of $\text{FePb}_2(\text{P}_2\text{O}_7)(\text{PO}_4)$, recorded between (4000-400 cm^{-1}), is shown in Figure 2. Knowing the frequencies of normal vibration modes of the PO_4^{3-} ion in the isolated state and those relating to $\text{P}_2\text{O}_7^{4-}$ [19], we can interpret this spectrum as follows:

Bands centered at 1120, 1097 and 1018 cm^{-1} are tentatively attributed to valence antisymmetric and symmetric vibrational modes of $\text{P}_2\text{O}_7^{4-}$ groups and antisymmetric vibration of PO_4^{3-} ion. For the latter, the valence vibration band appears at 976 cm^{-1} . The valence vibration mode of POP bridge in $\text{P}_2\text{O}_7^{4-}$ ion is characterized by the presence of associated bands visible at 900 and 945 cm^{-1} . The band of a significant intensity at 742 cm^{-1} is

attributed to the deformation vibration mode of the $P_2O_7^{4-}$ ion. Remaining bands of lower intensities ($600, 570, 562, 544, 517, 483$ and 439cm^{-1}) are likely due to deformation vibrations of PO_4^{3-} and $P_2O_7^{4-}$ ions.

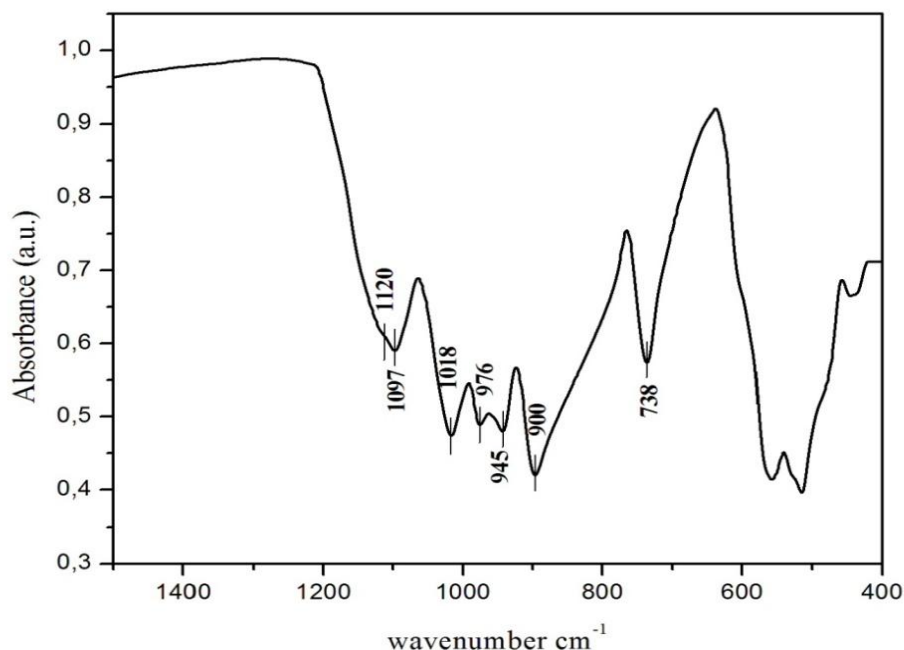


Figure 2: Infrared absorption spectrum of $FePb_2(P_2O_7)(PO_4)$

b-Raman scattering spectrum of $FePb_2(P_2O_7)(PO_4)$

The Raman scattering spectrum of $FePb_2(P_2O_7)(PO_4)$ is reported in Figure 3. It shows characteristic bands due to normal vibration modes of PO_4^{3-} ion and $P_2O_7^{4-}$.

The identification of the POP bridge is clearly demonstrated with Raman spectra showing a characteristic stretching vibration band at 756cm^{-1} and also the presence of valence vibration as well shown at 903 and 947cm^{-1} . Other bands of lower intensity may be due to external vibrations of PO_4^{3-} , $P_2O_7^{4-}$ ions and Fe-O and Pb-O bonds [20,21]. The vibration wavenumbers observed at $1146, 1107, 1066$ and 1036cm^{-1} correspond to valence symmetric and antisymmetric vibrations of the $P_2O_7^{4-}$ ion and antisymmetric vibrations of the PO_4^{3-} ion. The band located at 969cm^{-1} that is usually associated with the valence symmetric vibration of the PO_4^{3-} ion. However, we could not detect associated band for this vibration at 984cm^{-1} [22].

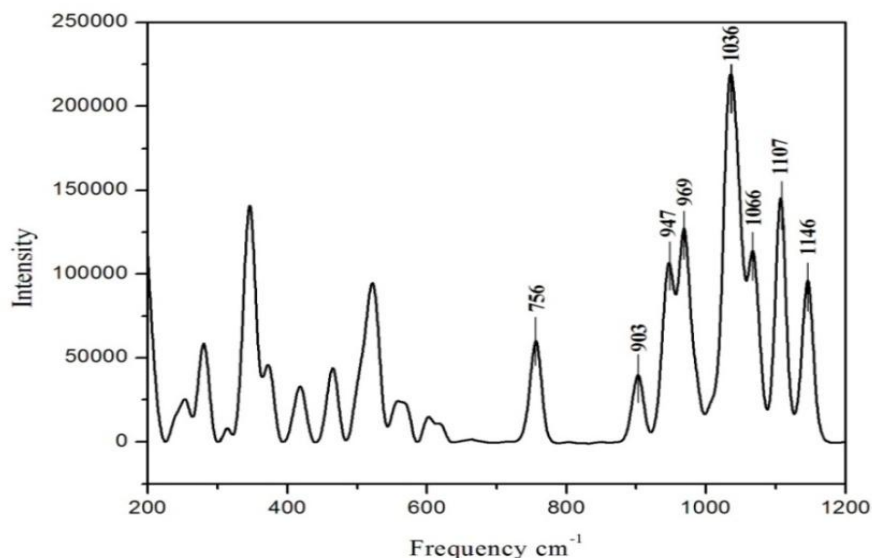


Figure 3: Raman scattering spectrum of $FePb_2(P_2O_7)(PO_4)$

We recall the results deduced from the site method technique indicating the presence of 18 active vibrations under IR radiation and 42 Raman active vibrations for both of PO_4^{3-} and $\text{P}_2\text{O}_7^{4-}$ groups. The data for the $\text{P}_2\text{O}_7^{4-}$ are summarized in the Table 3.

Table 3: Active vibrations for PO_4^{3-} and $\text{P}_2\text{O}_7^{4-}$ groups

Activity	Molecular group	Site group	Factor group
Raman	21	21	42
Infrared	17	21	42
Coincidence	17	21	0

From a simple comparison between the number of characteristic vibration bands using site method with experimental data from IR absorption and Raman scattering spectrum of $\text{FePb}_2(\text{P}_2\text{O}_7)(\text{PO}_4)$, we can't find a perfect correspondence. However, the distribution between different types of vibrations as a function of each group is more or less respected. Accordingly, we can conclude that the correlation effect is consistent with the obtained results on this material.

3.2. Mössbauer spectrum

Mössbauer spectroscopy is a very sensitive technique as it may lead to the electronic state of the active metal atom namely Iron in our materials. The present work reports the study by Mössbauer spectroscopy of $\text{FePb}_2(\text{P}_2\text{O}_7)(\text{PO}_4)$ solid obtained after calcination. The paramagnetic states shown in Figure 4, the room temperature spectrum has been fitted by least square method with one Lorentz-type doublet. The obtained parameters are listed in Table 4.

Table 4: Mössbauer parameters determined on $\text{FePb}_2(\text{P}_2\text{O}_7)(\text{PO}_4)$ at 290K.

Site	δ (mms ⁻¹) ± 0.002	Δ (mms ⁻¹) ± 0.002	Γ (mms ⁻¹) ± 0.01
Fe ³⁺ (4e)	0.45	1.09	0.27

The isomer shift value is characteristic of high spin Fe^{3+} in an octahedral oxygen environment [23]. Their relatively high amplitudes probably originate from the rather high ionicity of the Fe-O bond: the high polarizing P atom withdraws electronic density on the P-O bond. This is in agreement with the previous structural information: (P-O)-Fe distances are shorter than the (P-O)-P. The room temperature values are closed to those observed for another phosphates (e.g., $\delta = 0.45$ for NaFeP_2O_7 [12]; $\text{Na}_3\text{Fe}_2(\text{PO}_4)_3$ [24] and $\text{Fe}_3(\text{P}_2\text{O}_7)_2$ [25]). The antiferromagnetic state: At 4.2K, the spectrum displays a typical sextet of ion Fe^{3+} (as shown in Figure 5 which confirms that the magnetic order takes place at this temperature (See magnetic measurement)). The obtained parameters are given in the Table 5.

Table 5: Mössbauer parameters at 4K.

Site	δ (mms ⁻¹) ± 0.002	Δ (mms ⁻¹) ± 0.002	Γ (mms ⁻¹) ± 0.01	H (KOe) ± 1
Fe ³⁺ (4e)	0.54	-0.68	0.47	527

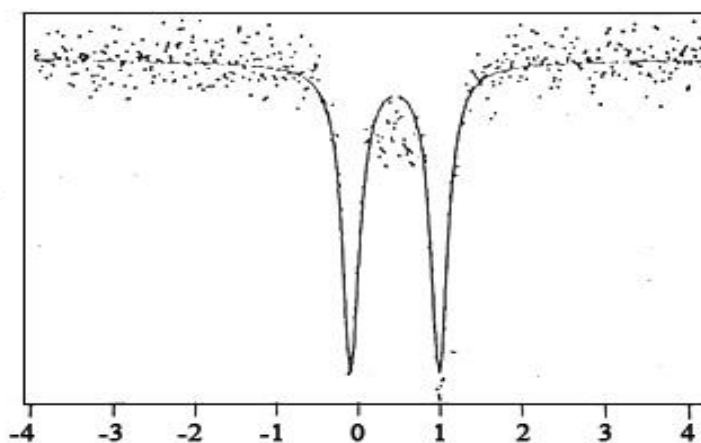


Figure 4: Mössbauer spectra at T= 290 K

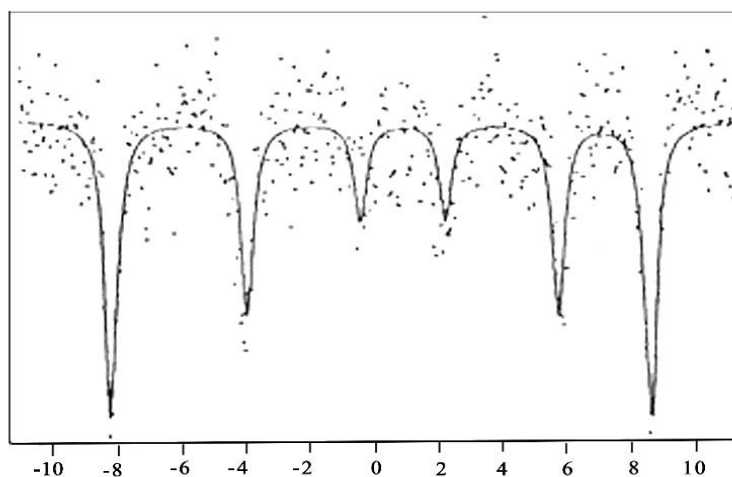


Figure 5: Mössbauer spectra at T=4K

3.3. ^{31}P NMR spectroscopy.

In order to deeply elucidate the phosphorus environment, convenient and specific tool using ^{31}P NMR spectroscopy is applied to analyze the $\text{FePb}_2(\text{P}_2\text{O}_7)(\text{PO}_4)$ material.

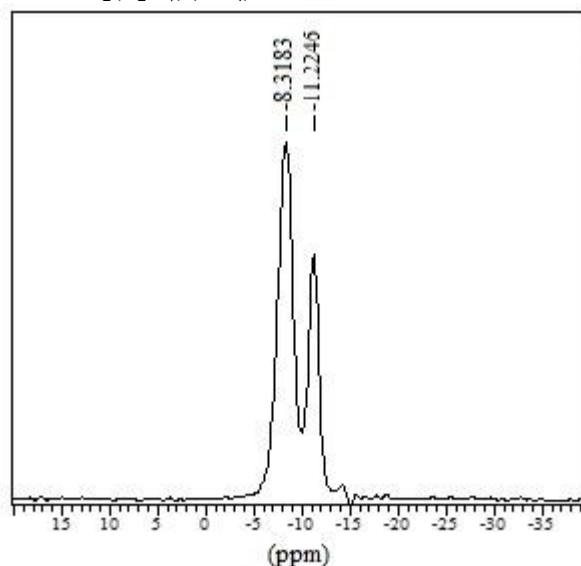


Figure 6: ^{31}P NMR patterns of $\text{FePb}_2(\text{P}_2\text{O}_7)(\text{PO}_4)$.

Figure 6 shows ^{31}P NMR spectrum of $\text{FePb}_2(\text{P}_2\text{O}_7)(\text{PO}_4)$ solid phosphate. Two distinct signals appear at - 11.224 ppm and - 8.318 ppm shift positions, the NMR signals may tentatively be assigned to PO_4 and P_2O_7 differing sites of phosphorus [26]. This finding confirms the results determined by XRD, IR and Raman revealing the presence of P-O and P-O-P chain based configurations of phosphate groups in $\text{FePb}_2(\text{P}_2\text{O}_7)(\text{PO}_4)$ structure.

Conclusions

Single crystals of a new $\text{FePb}_2(\text{P}_2\text{O}_7)(\text{PO}_4)$ mixed phosphate compound were synthesized using $\text{Fe}(\text{NO}_3)_3 \cdot 9\text{H}_2\text{O}$, $\text{Pb}(\text{NO}_3)_2$ and $\text{NH}_4\text{H}_2\text{PO}_4$ as starting materials and a progressive thermal treatment up to 900°C in air. The single crystals were evidenced by means of crystal structure analysis using XRD, and vibrational analysis using FTIR and Raman spectroscopy. The iron (III) state was characterized using Mössbauer technique and ^{31}P NMR spectroscopy demonstrated the coexistence of two distinct phosphorus sites inside the mixed phosphate structure in accordance with the Raman and IR observations.

References

1. Gleitzer C., *Eur. J. Solid State Inorg. Chem.*, 28 (1991) 77.
2. Bonnet P., Millet J.M.M., Leclercq C., and Védrine J.C., *J. Catalysis*, 158 (1996) 128-141.

3. Goodenough J.B., Hong H.Y.P., Kafalas J.A. *Mater. Res. Bull.* 11 (1976) 173.
4. Polles F., Parent C., Olazcuaga R., Le Flem G., Hagenmuller P., *C.R. Acad. Sci. Paris 306 serie II*, (1988) 765.
5. Corbridge D.E.C., *Elsevier, Amsterdam*, (1974).
6. Haushalter R.C., Mundi L.A., *Chem. Mater.*, 4 (1992) 31.
7. Clearfield A., *Chem. Rev.*, 88 (1988) 125.
8. Gleitzer C., *Eur. J. Inorg. Chem.*, 28 (1991) 77-91.
9. Durif A., *Crystal Chemistry of Condensed Phosphates Plenum, New York*, (1995).
10. Bouffessi A., Boukhari A., Holt E. M., *Acta Cryst. C* 52 (1996) 1594-1597.
11. Le Caer G., *Private Communication*.
12. Terminiello L., Mercader R. C., *Hyperfine Interact.*, 50 (1989) 651.
13. Battle P. D., Cheetham A. K., Harrison W.T. A., Long G. J., *J. Solid State Chem.*, 62 (1986) 16.
14. Kwang-Hwa LII, *J. Chem. Soc. Dalton Trans.*, 819 (1996).
15. Halford R.S., *J. Chem. Phys.*, 14 (1946), 8-15.
16. Horning D.F., *J. Chem. Phys.*, 16 (1948) 1063-1076.
17. Winston H., Halford R.S., *J. Chem. Phys.*, 17 (1949) 607-616.
18. Herzberg G., *Infrared and Raman spectra of Polyatomic Molecules, Van Nostrand* (1946).
19. Harcharras M., Ennaciri A., Rulmont A., Gilbert B., *Spectrochimica Acta* 53A (1977) 345.
20. Nakamoto K., *Infrared Spectra of Inorganic and Coordination Compounds, John Wiley and Son, Inc. New York, London*.
21. Mizrahi A., Wingnacourt J.P., Steinfink H., *Journal of Solid state Chemistry* 133 (1977) 516.
22. A. Oulmekki, « *Contribution à l'étude du système M-P-O : synthèse, structure et propriétés physico-chimiques des nouveaux phosphates $FePb_2(P_2O_7)(PO_4)$, $Fe_2Pb_3(PO_4)_4$, $MgFe_2(P_2O_7)_2$, $CoFe_2(P_2O_7)_2$, $Co_5Fe_2(P_2O_7)_4$* », Faculté des sciences Oujda. Thèse (2002).
23. Elbouaanani L. K., Malaman B., Gérardin R., *Journal of Solid state Chemistry* 147 (1999) 000-000.
24. Beltran-Porter D., Olazcuaga R., Fourens L., Menil F., Le Flem G., *Rev. Phys. Appl.*, 15 (1980) 1155.
25. Ijjaali M., Venturini G., Gerardin R., Malaman B., Gleitzer C., *Eur. J. Solid State Inorg. Chem. t.* 28 (1991) 983.
26. Castets A., « *RMN de matériaux paramagnétiques: mesure et modélisation* », PhD thesis, November (2011).

(2017) ; <http://www.jmaterenvironsci.com>